Magnesium Technology 2013
Edited by: Norbert Hort, Suveen N. Mathaudhu, Neale R. Neelameggham, and Martyn Alderman
TMS (The Minerals, Metals & Materials Society), 2013

Increasing volume fraction of precipitates and strength of a Mg-Zn-Y alloy by pre-ageing deformation

Julian M Rosalie[1], Hidetoshi Somekawa[1], Alok Singh[1], Toshiji Mukai[2]

[1]Structural Materials Unit, National Institute for Materials Science, Tsukuba, 305-0047, Japan.
[2]Dept. Mechanical Engineering, Kobe University, 1-1 Rokkodai, Nada, Kobe city, 657-8501 Japan.

Keywords: Magnesium-zinc-yttrium; Precipitation; Microstructure; Transmission electron microscopy

Abstract

Pre-ageing deformation was applied to a Mg-Zn-Y alloy to refine the size of β_1' precipitates. Reductions in the precipitate length and diameter were accompanied by a substantial increase in the volume fraction of the β_1' precipitates from 0.5% (no pre-strain) to 2.3% (5% pre-strain). This contrasted with Mg-Zn alloys, in which the precipitate volume fraction in the peak aged condition was not affected by pre-ageing strain. The increase in precipitate volume fraction contributed significantly to an increase in the yield strength from 217 MPa (no pre-strain) to 286 MPa (5% pre-strain). Precipitate strengthening via Orowan looping was the most significant contributor to the overall strength of the alloy.

Introduction

Pre-ageing deformation is used to enhance the precipitation strengthening response in a wide range of alloys and has been shown to be effective in Mg-Zn alloys [1, 2]. These alloys derive their strength from the controlled precipitation of rod-shaped precipitates (termed β_1') which have the long axis parallel to $[0001]_{Mg}$. In a recent study on precipitation hardening of Mg-Zn alloys, it was found that the yield strength could be increased from 273 MPa with T6 heat treatment (solution treatment plus artificial ageing) to 309 MPa by using a T8 treatment (solution treatment, cold-work and artificial ageing) using only 3-5% pre-ageing deformation [2]. This improvement in yield strength was due to dislocations providing heterogeneous nucleation sites for β_1' precipitates, resulting in accelerated precipitation kinetics and a refinement of the precipitate size.

The rod-shaped β_1' precipitates also form in magnesium-zinc alloys containing yttrium and rare earth (RE) additions. These elements are used to improve the high-temperature properties of Mg-Zn alloys [3, 4] and minor additions significantly modify the equilibrium phase behaviour. Yttrium has negligible solid solubility in Mg [5] and partitions to the grain boundaries in the form of a grain boundary eutectic comprised of an icosahedral phase (i-phase, Mg_3Zn_6Y [6–9]) and Mg [10]. In alloys with Zn:Y ratios close to the stoichiometry of the i-phase, under equilibrium conditions, little remaining zinc is expected to be available for β_1' phase precipitation and the alloy should show minimal precipitation strengthening.

The present work set out to examine whether pre-ageing deformation could be applied to improve the precipitation strengthening of MgZnY alloys. This revealed the surprising observation of an increase in the β_1' precipitate volume fraction when pre-ageing strain was applied [11]. Here we discuss in greater detail the reasons behind this increase in the precipitate volume fraction of β_1' precipitates.

Experimental details

Billets with composition Mg-3.0at.%Zn-0.5at.%Y were prepared from pure elements via direct-chill casting. Mg (99.99%) was heated to 700°C under a CO_2 atmosphere. Once the temperature had stabilised, the required amount of Zn (99.999%) was added and the melt was stirred. Hydrogen was removed by bubbling CO_2 through the melt for 5 minutes, after which the melt was poured into a steel mold and allowed to cool. The compositions were confirmed via inductively-coupled plasma mass spectroscopy (ICP-MS). The billets were homogenised for 15 h at 350°C and extruded into 12 mm diameter rods at 300°C with an extrusion ratio of 12:1. Tensile samples of gauge length 15 mm and diameter 3 mm were machined from the extruded rods.

The tensile samples were given a T8 heat treatment comprised of a solution-treatment followed by cold-work and isothermal ageing. Samples were encapsulated in argon, solution treated for 1 h at 400°C and and quenched into water at room temperature. Pre-ageing deformation was carried out by straining the tensile samples to a nominal plastic strain of 3%

or 5% on an Instron mechanical tester. Tensile deformation was applied parallel to the extrusion axis at a strain rate, $\dot{\epsilon}$, of $1 \times 10^{-3}\,\mathrm{s}^{-1}$. Sections of both solution treated and deformed samples were polished and etched with an acetic picral reagent for examination by light microscopy. The remaining samples were then aged to peak hardness in an oil bath at 150°. Maximum hardness was reached after 216-256 h for T6 treatments samples and 32-48 h for T8 treatments. Tensile tests were repeated in the Instron mechanical tester, with three samples for each condition strained to failure at the same strain rate of $1 \times 10^{-3}\,\mathrm{s}^{-1}$.

Solution-treated and quenched samples were polished for examination using electron back-scattered diffraction (EBSD) on a field emission scanning electron microscope. EBSD data was analysed using OIM Analysis software, version 6.1.

The β_1' precipitate size and spacing in T6 and T8 samples were determined in the peak-aged condition. Samples for TEM analysis were prepared by grinding to $\sim 70\,\mu$m and thinning to perforation using a Gatan precision ion polishing system. TEM observations were conducted using JEOL 4000EX and 2100 instruments operating at 400 kV and 200 kV, respectively. Stereological measurements utilised ImageJ software version 1.44.

Results

Grain structure

Optical micrographs showed a microstructure consisting of equiaxed grains with coarse intermetallic particle which formed chains in the extrusion direction. A grain size of $17 \pm 3\,\mu$m was measured using line intercepts. Twinning was extremely limited, with only 1-3% twins by volume fraction measured by point counting. As this value was independent of the pre-ageing deformation (up to 5%) it is thought that this most likely represents a sample-processing artifact. A solution-treated sample was also examined using electron back-scattered diffraction (EBSD) and twins were not detected. An average grain size of $14 \pm 1\,\mu$m was calculated using EBSD measurements of the grain diameter.

Precipitate size and distribution

The precipitate size and distribution was strongly affected by pre-ageing deformation. In non-deformed samples the microstructure in the peak-aged condition consisted of rod-like β_1' precipitates, a smaller fraction of β_2' plates on the basal planes and coarse spheroidal precipitates. The spheroidal precipitates are consistent with previous reports of i-phase particles in Mg-Zn-Y alloys [12]. Figure 1 shows electron micrographs taken with beam normal to the hexagonal axis of the matrix. Electron micrographs obtained with the beam along the hexagonal axis (Figure 2) showed the rod-like β_1' precipitates in cross-section and indicated that the precipitates were sparse and well-separated.

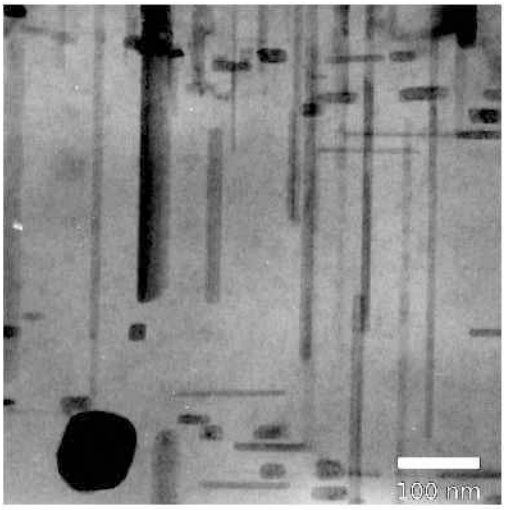

(a) 0% strain

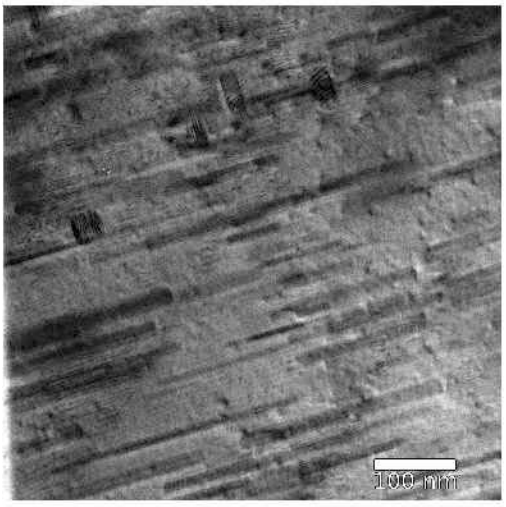

(b) 5% strain

Figure 1: Transmission electron micrographs of β_1' precipitates in the peak aged condition after a) T6 treatment and (b) T8 treatment with 5% pre-strain. The T6 sample contains a large, spheroidal i-phase particle. The beam direction is normal to the c-axis of Mg and to the long axis of the β_1' precipitates.

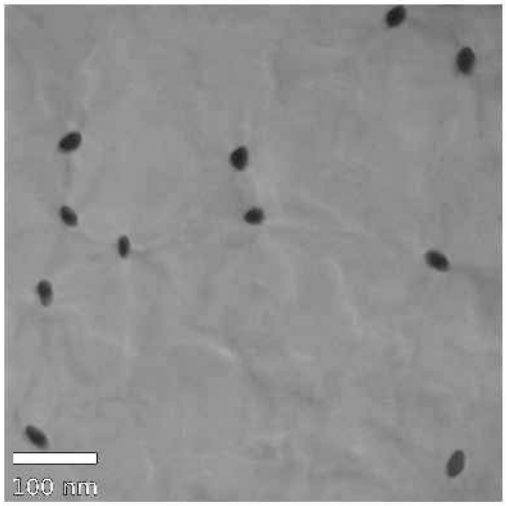

(a) 0% strain

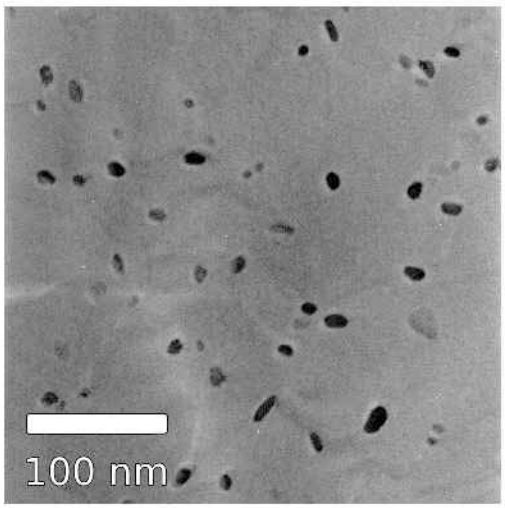

(b) 5% strain

Figure 2: Transmission electron micrographs of β_1' rod-shaped precipitates in the peak aged condition after a) T6 treatment and (b) T8 treatment with 5% pre-strain. The beam direction is parallel to the c-axis of Mg and the β_1' precipitates are viewed in cross section. Note that the pre-strained sample is shown at higher magnification in order to make the smaller β_1' preciptitates visible.

In samples given 3–5% pre-ageing strain the number of plate-like β_2' precipitates was less substantial and the spheroidal ternary phase precipitates were extremely rare. The length of the rod-like precipitates was substantially reduced as can been seen in Figure 1(b). When viewed along the hexagonal axis the β_1' precipitates were were found to be smaller in diameter and more closely spaced (Figure 2(b)).

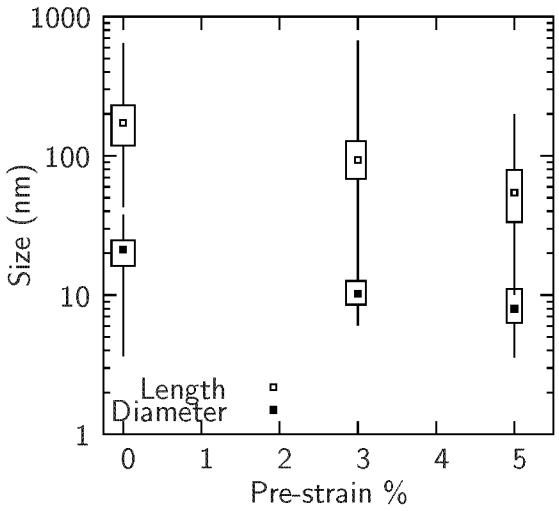

Figure 3: Precipitate length and diameter as a function of pre-ageing deformation. The boxed region contains 50% of of the precipitate length values, with the lines indicating the full range of values.

The distribution of β_1' precipitate lengths and diameter is summarised in Figure 3. Filled (open) squares show the mean diameter (length) of the precipitates. T6-treated samples had a average β_1' precipitate length of 475 nm. This was reduced to an average of 67 nm when 5% pre-strain was applied. The boxed region of the plot indicates the range containing 50% of the precipitate length values, with the line indicating the range of measured values. Precipitates were able to grow to lengths of >600 nm in T6 samples.

The volume fraction of β_1' precipitates was determined from measurements of precipitate length, diameter and number density. The volume fraction of precipitates in Mg-Zn was approximately 3.5% regardless of the level of pre-ageing deformation. The volume fraction of precipitates in non-deformed (T6 treated) Mg-Zn-Y was only 0.5%, due to the low number density of precipitates (as indicated in Figure 2(a)). The application of either 3% of 5% pre-strain increased the volume fraction substantially to 2.3%. The contrasting behaviour indicates that dislocations introduced prior to deformation in the ternary alloy not only accelerate the nucleation kinetics, but in MgZnY these dislocations also modify the partitioning of zinc solute.

Tensile properties

Isothermal ageing substantially increased the yield strength (σ_y), with the improvement more pronounced in the alloys strained before ageing. Stress-

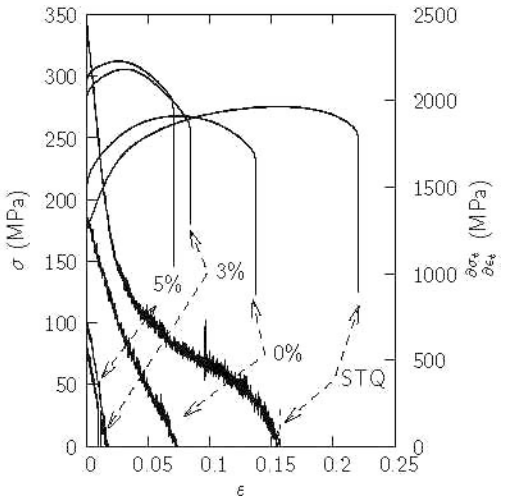

Figure 4: Stress-strain curves (left) and hardening rate curves (right) for various levels of pre-ageing deformation. "STQ" indicates the solution-treated and quenched condition in which β_1' precipitates were absent. Other samples were tested in the peak-hardness condition.

strains curves and hardening rate curves for uniaxial tension are provided in Figure 4. T6 treatment increased the yield strength by ~50% from 150 MPa to 217 MPa. T8 treatments resulted in further increases to σ_y to 281 MPa for 3% pre-strain and a slight further increase to 287 MPa for 5% strain.

The hardening rate curves (Figure 4) showed that the alloy work-hardens in all heat-treatment conditions examined. Work-hardening was most significant in the solution-treated and quenched sample, in which precipitates were absent and zinc was present in solid-solution. In T6 treated samples the work-hardening rate was ~1350 MPa at the yield point and decreased with further deformation. Work-hardening also occurred for T8-treated samples, with hardening rates of 750 MPa at the yield point and no significant difference between samples deformed 3% and 5% prior to ageing.

Discussion

The increase in the volume fraction of β_1' precipitates due to pre-ageing strain is an unusual feature and one that is not present in Mg-Zn alloys. This effect arises from the low solid solubility of yttrium and competition between i-phase and β_1' precipitation. The alloy composition has a Zn:Y ratio of 6:1, which falls within the two phase Mg + i-phase (Mg_3Zn_6Y) region of the Mg-Zn-Y phase diagram [9]. Under equilibrium heat-treatment condition the microstructure would be expected to consist of a Mg-rich matrix, with i-phase forming a grain boundary network.

During solution treatment there is substantial solid solubility for zinc whereas yttrium remains virtually insoluble. Consequently, at the commencement of isothermal ageing there is substantial excess Zn within the grains. If this solute is able to diffuse to the grain boundaries it will be incorporated into the grain boundary i-phase. However, the dislocations introduced by pre-ageing deformation act as preferred nucleation site for β_1' precipitates, as is the case in Mg-Zn binary alloys [2]. These defects act as solute-traps, precipitating the solute in the form of the rod-like particles, before it is able to reach the grain boundaries.

The fact that it is possible to precipitate β_1' particles at the expense of the i-phase highlights the difficulty in precipitating the icosahedral phase. Previous attempts to use the icosahedral phase to strengthen Mg alloys using i-phase particles have been forced to resort to severe plastic deformation (e.g. equal channel angular extrusion (ECAE) [13])to distribute yttrium more homogeneously through the alloy.

Strengthening mechanism

The increase in the yield strength of the alloys can be attributed almost entirely to precipitation strengthening, as is to be expected from the 32% increase in the yield strength obtained through isothermal ageing.

Extrusion was used primarily to introduce texture to the alloy, preventing twinning during pre-ageing deformation, rather than to provide significant grain refinement. This was advantageous from an experimental perspective as it simplified quantification of the precipitate size and number density using TEM. The large grain size (14μm from EBSD measurements) that resulted was responsible for the low base strength of the material. Based on the Hall-Petch plots for AZ and MgZnY magnesium alloys in tension [13–15] an alloy with grain size 14-17μm should have a base yield strength in the range of 160 MPa, close to the value of 150 MPa measured for solution-treated and quenched Mg-Zn-Y (Figure 4).

Despite the use of pre-ageing deformation, work hardening was also not a significant contributor to the mechanical properties. Temperatures sufficient to precipitate β_1' particles within 32–48 h for T8 samples are also within the temperature range used from strain relief of ZK alloys [16]. Previous studies [2, 11]

noted a rapid decrease in the hardness during the first 1 h of ageing that was attributed to the annealing out of dislocations. Since ageing times of 24-32 h were required to reach peak hardness with T8 treatments it is probable that the dislocation density is low and that strain hardening is negligible.

Solid-solution strengthening was thought to add contribute slightly to the overall strength of the alloy. If the Zn content is assumed to be the equilibrium value at the ageing temperature (T6 and T8 samples), then the contribution from solid solution strengthening can be determined from the equation [17]: $\Delta\sigma = \sqrt{2}m\mu\epsilon^{3/2}c^{1/2}$where σ is the yield strength, m is the Taylor orientation factor (3 in Mg), μ Shear modulus, ϵ is the misfit strain (0.17 for Zn in Mg) and c is the solute concentration [18] (given in at.%). This gives a value of 12 MPa for solid solution strengthening in the peak-aged condition.

With minimal grain boundary strengthening and in the absence of significant work-hardening and solid-solution strengthening, the increase in the strength of the alloy by 67 MPa (T6 treatment) or 125–131 MPa (T8 treatment) should be attributable to precipitation of the β_1' particles.

Conclusions

- Solution-treatment and ageing (T6 treatment) of Mg-Zn-Y resulted in the precipitation of a volume fraction of approximately 0.5% β_1' precipitates, substantially less than the value of approximately 3.5% in a Mg-Zn alloy given similar treatment. This resulted in a weak precipitation strengthening response.

- Solution-treatment, pre-strain and ageing (T8 treatment) introduced dislocations that provided heterogeneous nucleation sites for β_1' precipitates. These defects acted as solute traps for Zn, reducing the amount of solute that diffused to the grain boundaries. This increased the volume fraction of β_1' particles to approximately 2.3% while simultaneously refining the size of the β_1' precipitates.

- These effects combined to increase the yield strength by 32% from 217 MPa (no pre-strain) to 286 MPa (5% pre-strain). This was a greater relative increase than reported in Mg-Zn alloys, where 5% deformation increased yield strength by ∼15%.

References

[1] L. Sturkey, J. B. Clark. Mechanism of age-hardening in magnesium-zinc alloys. *J. Inst. Mater.*, **88**:(1959-60) 177.

[2] J. M. Rosalie, H. Somekawa, *et al.* The effect of size and distribution of rod-shaped precipitates on the strength and ductility of a Mg-Zn alloy. *Mater. Sci. Eng. A*, **539**:(2012) 230.

[3] C. J. Boehlert. The tensile and creep behavior of Mg-Zn alloys with and without Y and Zr as ternary elements. *J. Mater. Sci*, **42**:(2007) 3675.

[4] Y. Li, F. Xu, *et al.* Influence of Y element on microstructure and mechanical properties of ZK60 alloy. *Adv Mater Res*, **284-286**:(2011) 1568.

[5] G. Shao, V. Varsani, *et al.* Thermodynamic modelling of the Y-Zn and Mg-Zn-Y systems. *CALPHAD*, **30**(3):(2006) 286.

[6] J. P. Hadorn, K. Hantzsche, *et al.* Role of solute in the texture modification during hot deformation of Mg-rare earth alloys. *Metall. Mater. Trans. A*, **43A**(4):(2012) 1347.

[7] L. Y. Wei, G. L. Dunlop, *et al.* Precipitation hardening of Mg-Zn and Mg-Zn-RE alloys. *Metall. Mater. Trans. A*, **26A**(7):(1995) 1705.

[8] A. Singh, A. P. Tsai. Structural characteristics of β_1' precipitates in Mg-Zn-based alloys. *Scr. Mat.*, **57**:(2007) 941.

[9] A. P. Tsai, A. Niikura, *et al.* Highly ordered structure of icosahedral quasicrystals in Zn-Mg-RE (RE= rare earth metals) systems. *Philos Mag Lett*, **70**(3):(1994) 169.

[10] A. P. Tsai, Y. Murakami, *et al.* The Zn-Mg-Y phase diagram involving quasicrystals. *Philos. Mag. A*, **80**(5):(2000) 1043.

[11] J. M. Rosalie, H. Somekawa, *et al.* The effect of precipitation on strength and ductility on Mg-Zn-Y alloys. *J. Alloys Comp.*

[12] A. Singh. Phase relations, formation and morphologies in Mg-Zn-RE (RE=Y, rare earth) alloys. in M. O. Pekuleryuz, N. R. Neelameggham, *et al.*, eds., *Magnesium Technology*, 337–342, The Minerals, Metals and Materials Society, New Orleans, 2008.

[13] A. Singh, M. Watanabe, *et al.* Microstructure and strength of quasicrystal containing extruded Mg-Zn-Y alloys for elevated temperature application. *Mater. Sci. Eng. A*, **385**:(2004) 382.

[14] D. H. Bae, S. H. Kim, *et al.* Deformation behavior of Mg-Zn-Y alloys reinforced by icosahedral quasicrystalline particles. *Acta Mater.*, **50**(9):(2002) 2343.

[15] E. Mora, G. Garcés, *et al.* High-strength Mg-Zn-Y alloys produced by powder metallurgy. *Scr. Mat.*, **60**(9):(2009) 776.

[16] M. M. Avedesian, H. Baker, eds., *Magnesium and magnesium alloys*, 79, ASM speciality handbook, ASM, 1999.

[17] Y. Chino, M. Kado, *et al.* Compressive deformation behavior at room temperature-773k in Mg-0.2 mass%(0.035at.%)Ce alloy. *Acta Mater.*, **56**:(2002) 387.

[18] J. B. Clark, L. Zabdyr, *et al.*, *Binary alloy phase diagrams*, chap. Mg-Zn (Magnesium-Zinc), 2571–2572, ASM International, 1988.